HIGH PRECISION AND HIGH THROUGHPUT SURFACE STRUCTURING BY SYNCHRONIZING MECHANICAL AXES WITH AN ULTRA SHORT PULSED LASER SYSTEM IN MOPA ARRANGEMENT

Paper M1207

Beat Jaeggi[1], Beat Neuenschwander[1], Urs Hunziker[1], Joseph Zuercher[1], Thomas Meier[2], Markus Zimmermann[2], G. Hennig[3]

[1] Bern University of Applied Science, Institute of Applied Laser, Photonics and Surface Technologies, Pestalozzistrasse 20, 3400 Burgdorf, Switzerland
[2] Bern University of Applied Science, Institute for Mechatronic Systems, Pestalozzistrasse 20, 3400 Burgdorf, Switzerland
[3]Daetwyler Graphics, Flugplatz, 3368 Bleienbach, Switzerland

Abstract

For surface and 3D structuring ultra short pulsed laser systems are mostly used in combination with galvo scanners. This work reports on the synchronization of the scanner mirror motion with the clock of the laser pulses, which is usually in the range of 100 *kHz* up to several MH, by a modification of the electronic scanner control. This synchronization facilitates the placement of the small ablation craters from single pulses during the mirror motion with the precision of about 1 μm relative to each other. The precise control of the crater positions offers the possibility to test and optimize new structuring strategies. Results of this optimization process with respect to minimum surface roughness, steepness of wall, accuracy to shape and efficiency will be presented.

Introduction

A standard process for surface structuring applications is the filling of a given outline with a parallel hatching. Commonly 3D structures are built up in a 2.5D process by a series of slices and by adapting the outline and the hatch angle from slice to slice. The lines of the hatch pattern are generated with mechanical axes, usually galvo scanners, and the laser pulse train is switched on and off via an external modulator which is gated by a signal from the axes control software. Fig. 1 shows the different situations that can appear at the border of a structure. If the pulse train is switched on with the start of the axes acceleration the distance from pulse to pulse (pitch) increases until the axes has reached its final speed (fig. 1a). Such lines show deep marks at the start and ending points of the single lines but the effective position of these points are well defined. To avoid this phenomenon of deep marking a so called sky-writing option can be used. Sky-writing means that the axes already have the correct velocity at the beginning of the marking. With the sky-writing option a displacement of the start position of plus/minus the distance between two consecutive pulses has to be accepted (fig. 1b). Therefore for high precision structuring applications this combination suffers from inaccuracies due to the asynchronous motion of the axes relative to the pulse train. If this problem should be avoided it will be necessary to synchronize the axes motion onto the output pulse train of the laser system or vice versa (fig. 1c). In the case of a Q-switched laser system the pulse train can be shifted by the external control software. This is a simple solution and is e.g. supported by many scanner control software. Currently in industrial applications ultra short pulsed laser systems will be used if high requirements concerning accuracy, defined surface roughness and small heat affected zone are demanded. Unfortunately with Q-switched laser system the achievable pulse durations are not short enough for this very precise micro-processing.

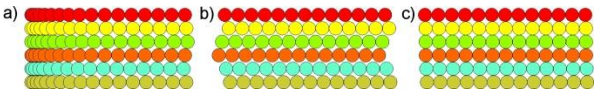

Fig. 1: Start positions of the different strategies: a) standard setup without sky-writing option; b) standard setup with the sky-writing option; c) synchronized system.

The today available industrially suited ultra short pulsed systems are turnkey systems, set up in a master oscillator power amplifier (MOPA) arrangement with a passively mode locked seed laser, followed by a pulse picker and a rod or disk amplifier to prepare the output pulse train. However, a MOPA design mostly has at the beginning of the amplifier chain a passively mode locked seed laser. Also the value of the pulse repetition rate can be chosen it might be a risky task to shift the

pulse train with the first pulse picker located directly after the seed oscillator. Risky because a change in the time interval between two consecutive pulses leads to a variation of the energy of the first or the first few pulses, known as first pulse problem. One possibility to overcome this is to tune the gating module and the followed mechanical components on the laser pulse train.

Synchronization

The standard laboratory setup includes control software and a controller board that controls the scan head and the POD-module, as seen in fig. 2.

The movements of the scanner are written into an instruction list on the controller board with the control software. The instruction list is then executed according to a software or hardware trigger. Depending on the type of movement the controller enables the POD.

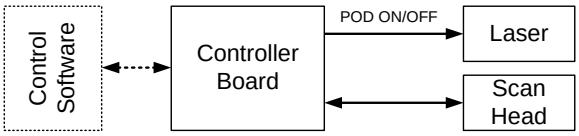

Fig. 2: Standard Laboratory Setup

As mentioned above it is not possible to modify the phase of the laser frequency. Therefore the scanner's movements have to be synchronized with the laser pulses. Fig. 3 shows the structure developed to synchronize the scanner movements with the laser pulses.

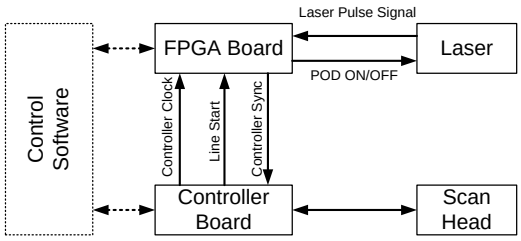

Fig. 3: Synchronized Setup

Since the execution of the commands in the instruction list depends on the controller clock, which can be modified with the controller sync entry, it is possible to lock the phase of the controller clock to the laser pulse signal. The phase detector and the filter of this phase locked loop were implemented in a Field Programmable Gate Array (FPGA) and the controller sync signal is generated by a controlled oscillator.

In order to create three dimensional structures black-and-white images are provided to the control software. The images are divided into lines and transmitted to the FPGA. Accordingly a linear movement is included into the instruction list. The start of the scanner movement is communicated to the FPGA and the laser pulses is enabled (white parts of the image) or not (black parts of the image).

Experimental Set-Up

As a source for the laser pulses a DUETTO system (Time Bandwidth Products) generating 10 *ps* pulses at 1064 *nm* wavelength was used. Afterwards the pulses were converted to a wavelength of 532 *nm* by second harmonic generation. The repetition rate is ranging from 50 *kHz* to 1 *MHz*. The energy per pulse is up to 200 μJ. The used scanner system was an IntelliScan 14 of Scanlab. The laser beam was circular polarized using a $\lambda/4$-plate and directed through 4 mirrors and a variable beam expander onto the galvo scanner. With a 100 *mm* telecentric f-theta objective the beam was focused to a spot radius of $w_0 = 5.7\ \mu m$, which was measured with a slit scanning beam profiler. Additionally a beam quality $M^2 \leq 1.1$ was measured, and therefore a Gaussian shaped beam could be assumed. All experiments were performed with the target surface in the focal plane of the telecentric f-theta objective. The analyzed sample material was copper Cu-DHP (in US: C12 200) whose surface was polished with a diamond suspension. The structures were measured by using a laser scanning microscope, a light optical microscope and a scanning electron microscope. To determine the achieved surface roughness and the taper angle, squares with a side length of 1 *mm* were machined. To present the limits of the system concerning minimum structure dimensions, bars and pillars with different side length were machined. To compare the achieved results, structures with the asynchronous system were machiend, as well. In this case the scanner movements were controlled by the Laserdesk-software of Scanlab.

Theoretical Background and Laserparameters

For high precision micro machining the material parameters are important. As a consequence of the two-temperature-model which is discussed in the literature [1-5], the ablation depth logarithmically depends on the applied fluence. For a Gaussian shaped beam the maximum ablation depth in the centre of the ablated crater therefore depends on the peak laser fluence F_0 in the beam centre by [5-12]:

$$z_{abl} = \delta \cdot \ln\left(\frac{F_0}{F_{th}}\right) \qquad (1)$$

The ablation depth z_{abl} thus depends on the two material parameters penetration depth δ and threshold fluence F_{th}. The threshold fluence F_{th} describes the minimum energy which is needed to ablate material. The penetration depth δ is the ability of the energy to penetrate into the material. With equation 1, and assuming a Gaussian beam shape, the ablated volume per pulse is then given by [9-12]:

$$\Delta V = \frac{1}{4} \cdot \pi \cdot \delta \cdot w_0^2 \cdot \ln^2\left(\frac{F_0}{F_{th}}\right) \qquad (2)$$

As shown in the literature [7-10,12], the removal rate can be maximized by choosing the optimum repetition rate at a given average power. From the expression for the optimum repetition rate and the maximum removal rate one can show that under best condition the ablated volume per pulse ΔV reads for a Gaussian beam and a top hat beam as well:

$$\Delta V = \pi \cdot w_0^2 \cdot \delta \qquad (3)$$

For a Gaussian shaped beam the peak fluence in the beam centre is given by the pulse energy and beam radius and reads:

$$F_0 = \frac{2 \cdot E_p}{\pi \cdot w_0^2} \qquad (4)$$

Comparing equations 2 and 3, and using the expression of the peak fluence (4) the optimum pulse energy E_p where the maximum removal rate is obtained is given by:

$$E_p = \frac{\pi \cdot w_0^2}{2} \cdot F_{th} \cdot e^2 \qquad (5)$$

With a given repetition rate f_{rep}, the average power P_{av} then reads:

$$P_{av} = E_p \cdot f_{rep} \qquad (6)$$

With the threshold fluence of 0.11 J/cm^2 and the penetration depth of 6.67 *nm*, which are determined for 512 pulses in an ablation study, the optimum pulse energy is 0.4 μJ. For a repetition rate of 100 *kHz* and 300 *kHz* the corresponding average power amounts 40 *mW* and 120 *mW*, respectively.

Results and Discussion

Scan Strategies

As a first task the best scan strategy for machining structures with a good result concerning the surface roughness and the optical effect was investigated. To compare the surface roughness the arithmetical mean roughness R_a was measured with the laser scanning microscope. The optical effect achieves the best value if no periodical structures appear. Due to the limitation of the synchronization software, it is possible to mark lines only in one direction. Scanning diagonal lines is not possible at the moment, and is subject of running investigations.

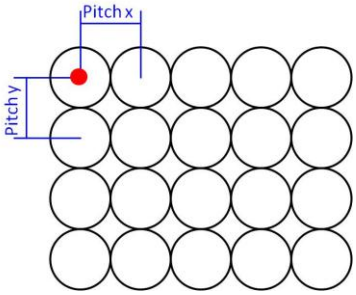

Fig. 4: Layer with the start position (red dot) and the pitches in x- and y-direction

To find the best strategy, squares with a side length of 1 *mm* and a constant number of layers were ablated. The design of the layer was always the same, i. e. a given pitch (distance between two consecutive spots) in both directions and a given starting point (red point in fig. 4). The first strategy was 120 layers, and 4 defined start positions. Each start position was addressed 30 times in the same sequence (1 to 4). The pitch was about 3 μm. Due to the multiple crossing of each position, periodical structures at the bottom of the structure could be observed. The second strategy was 120 layers as well, but with 120 different start positions, determined randomly with a uniformed distribution with the lower and upper endpoint of 0 and half of the pitch. The R_a-value decreases, because every layer starts with another start position and so the same position is addressed only once. But a periodical pattern at the bottom of the structure still rests. The periodical pattern disappeared at the same surface roughness when the uniformed random distribution of the start positions was changed to a normal or Gaussian distribution with the mean parameter μ of 0 and the standard deviation σ of a quarter of the pitch. Additional strategies with different arrangements of the pulses were tested. But always a periodical structure was observed. The best strategy found to be a

normal or Gaussian random distribution of the start positions.

Surface Roughness

The laser parameters were given by equation 5 and 6. The used average power was 40 *mW* by a repetition rate of 100 *kHz*. To find the optimal distance between two consecutive pulses (pitch in x- and y-direction) tests with different distances from 1/8 – 2 w_0 what conform to 0.75 μm to 12 μm, were done. With changing the distance, the whole absorbed energy changes when the number of layers is constant. Therefore the number of layers for a constant energy during the whole process has to be adjusted i.e. for a pitch of 1 μm, the number of layers was 13, for 3 μm 120 layers and for a pitch of 12 μm 1920 layers. Additionally to the squares machined with the synchronized set-up also the standard Laserdesk software was used. To guarantee the same pitch the hatch distance and the marking speed were chosen accordingly. Between two consecutive layers the hatch was turned around an angle of 15°.

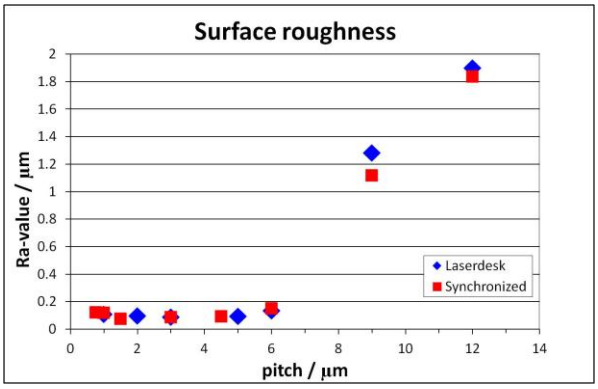

Fig. 5: A comparison of the achieved R_a-values versus the pitch

The lowest obtained surface roughness amounts about 90 *nm* for a pitch of about half of the spot radius. The minimum R_a-values of the synchronized structures (red dots in fig. 5) were in the same range as the values of the structures controlled with the Laserdesk software (blue points in fig. 5). In the region with a pitch of a half spot radius the surface roughness is nearly constant. With an increasing pitch, the overlap between two consecutive pulses disappeared, and the surface roughness increases as well.

Steepness of Wall

In the cross section view (fig. 6a) the definition of the taper angle is shown. The taper angle was measured at the same squares as the surface roughness. With the asynchronous system two different options can be chosen. With the sky-writing option (green dots in fig. 6b) the bottom close to the boundary of the structure has the same deepness as the rest of the structure (see fig. 7b). But the taper angle is even more flat caused by the different start positions of the lines showed in fig. 1b. Without the sky-writing option (red dots in fig. 6b), the taper angle increases, but deep marks on the ground can be observed (see fig. 7a). This is caused by the acceleration of the mirrors of the scanner. The increasing of the angle can be explained as follows: Due to the acceleration the pitch between two consecutive pulses is small. Therefore no big deviation of the start position appears. In the case of the sky-writing option, the deviation of the start position is plus/minus one pulse that means plus/minus the pitch, what equates a range of 6 μm. So the taper angle is lower (green dots in fig. 6b) but no acceleration marks appear (see fig. 7b). The synchronized system is a compromise of these two strategies. The taper angle is maximized to the values without the sky-writing (blue dots in fig. 6b) and no acceleration marks occur, see fig. 7c.

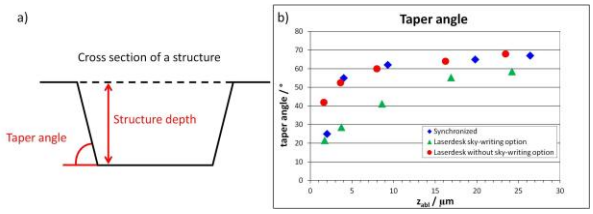

Fig. 6: a) Cross section of a structure; b) the taper angle versus the structure depth on the right side

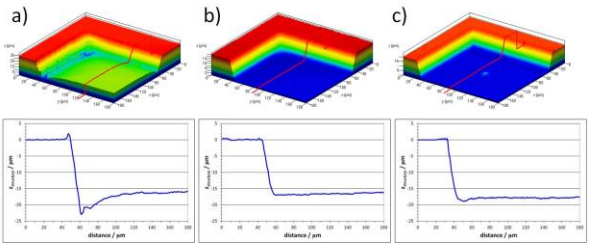

Fig. 7: Taper angle of a) Laserdesk software without sky-writing; b) Laserdesk software with sky-writing; c) Synchronized system; performed with 120 *mW*, 300 *kHz*, 3 μm pitch, 120 layers

Minimum Structures

For investigating the minimal obtainable structure dimensions a repetition rate of 300 *kHz* and an average power of 120 *mW* were chosen. The structures were performed with a pitch of 3 μm and 60 layers. Two different structures were examined: bars and pillars with a square horizontal projection. The minimal structure should still full fill the following two

conditions: first the height of the structure should be leveled with the surface. Second the horizontal projection in the case of the pillars should be squared. The minimum side length was always measured at the top of the structure. For the minimal bars a black-and-white bitmap with a pitch of 1 μm was used, but only every third pixel was shot. This strategy only works for 1-dimensional structures (like the bars) but not for pillars. To find the minimum structure dimension, bars with different web widths from 5 to 19 μm were produced. To compare the minimum bars with the Laserdesk software rectangles with a given distance between each rectangle were also machined. The hatched rectangles are built up of 60 layers and between two consecutive layers the hatch angle was turned around an angle of 3°. By increasing the distance between two rectangles from 1 μm to 30 μm the minimum bar can be estimated. In fig. 8a the minimal bars are shown for the process with the Laserdesk software without the sky-writing option on the left side. Fig. 8b shows the bars performed with the sky-writing option. The bar in the middle of this image achieves the condition for a minimum structure, defined at the beginning of this section. Fig. 8c shows the structures produced with the synchronized system. Also the bar in the middle reaches the condition for a minimum structure. The minimum web width for the synchronized system and the asynchronous shows values in the range of 3 to 5 μm, measured at the top of the structure. This corresponds to a minimum web width in the range between a half and one spot radius. The advantage of the synchronized system is the higher taper angle. Fig. 8d shows the periodical structure with the minimum bars performed with the synchronized system to show reproducibility.

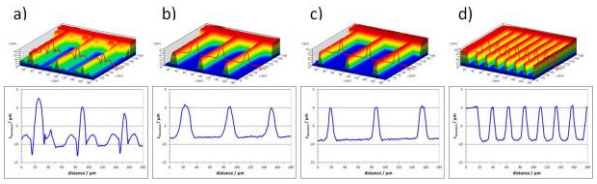

Fig. 8: Minimum bars controlled by a) Laserdesk without sky-writing; b) Laserdesk with sky-writing; c) synchronized system; d) periodical minimum bars; 120 mW, 300 kHz, 1 μm pitch, 60 layers

For the minimal pillars a black-and-white bitmap was created using a matlab routine. One Pixel equals one laser pulse. The structures were performed with a pitch of 3 μm and 60 layers. With the Laserdesk software the given outline of the pillars was filled with a hatch. The hatch distance was 3 μm and between two consecutive layers the hatch was turned around an angle of 3°. With increasing the side length of a pillar from 3 to 21 μm the minimum achievable pillar dimension can be estimated. In fig. 9a the minimum pillars for the Laserdesk software without the sky-writing mode are shown. There the typical marks due to the acceleration of the scanner mirrors are clearly seen. Fig. 9b shows the pillars produced with the sky-writing mode and fig. 9c the pillars from the synchronized system. The minimum side length of the squared horizontal projection, measured at the top of the structure was for both strategies in a range of about 6 μm, which corresponds more or less to the spot radius.

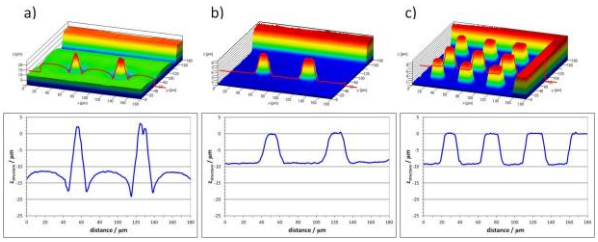

Fig. 9: Minimum pillars, controlled by a) Laserdesk without sky-writing; b) Laserdesk with sky-writing; c) synchronized system, 120 mW, 300 kHz, 3 μm pitch, 60 layers

Bitmaps

The synchronization software needs a black-and-white bitmap file. The bird shown in fig. 10, was machined from such a black-and-white image. The figure shows a comparison between a microscope image and the corresponding SEM image. In this experiment once the positive and once the negative form were machined. Fig. 11 shows some other examples of machined black-and-white. On the left hand side always the microscope image and on the right hand side the original black and white images are shown.

Gray scale images can be transformed into 3D information by the following procedure:

- The pixels with the highest and the lowest gray scale values denote the bottom and the top points in the 3D image.
- The range of the gray scale values defines the number of layers.
- A pixel with a gray scale value of N will be marked in layer N and in all consecutive layers.
- To control the number of machined layers the grayscale values can be scaled e.g. with matlab.

Fig. 12 illustrates this procedure for a grayscale picture of Tux [18]. On the left side (fig. 12a) the original grayscale picture is shown. A typically black-and-white layer is shown in the middle (fig. 12b) and the

finally machined image on the right side (fig. 12c). The structure was produced with 300 *kHz* repetition rate, 120 *mW* average power, a pitch of 3 μm and with 100 layers. The sequence of the single black-and-white bitmaps was produced by a simple matlab routine.

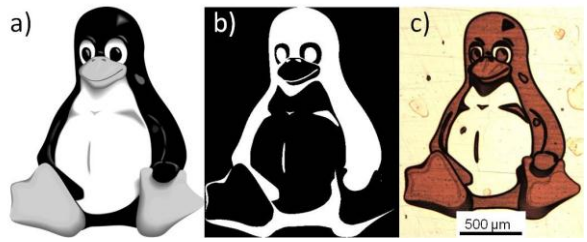

Fig. 10: Structure based on a grayscale image: a) original grayscale image [18]; b) typical black-and-white layer; c) microscope picture of the structure; machined with 120 *mW*, 300 *kHz*, 3 μm pitch, 100 layers

Fig. 13 shows another example, left the greyscale image [19] and a SEM image of the structure machined into copper. Right a detailed microscopic image showing a part of the hand.

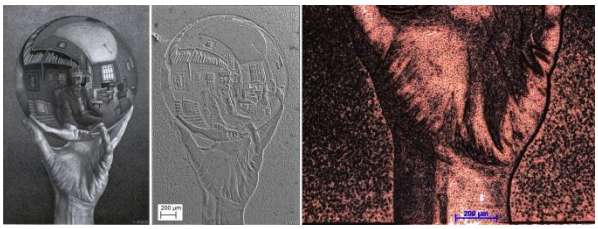

Fig. 13: Additional structure based on a grayscale image machined in copper. Left: original grayscale image [19] and SEM image. Right: Detailed image from optical microscopy

With a similar method also real 3D-data can be transformed into a sequence of black-and-white bitmaps to form a topographic image by laser machining. As an example, fig. 14b shows the topography of Switzerland, based on the real 3D-data [20] and machined with 447 different layers.

With the used laser system and the Laserdesk software it was not possible to generate bitmaps. The software generates a signal with a different voltage value for the different grayscale values. With this signal the laser output power can be changed. For our laser system only the laser on/off signal to control the POD-module is used, as seen in fig. 2. The laser output power cannot be adjusted during the process. Therefore a comparison was not possible.

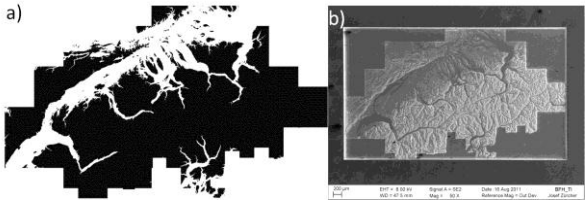

Fig. 14: Structure based on topography data of Switzerland [20] a) typical black-and-white layer; b) SEM image of the structure, 120 *mW*, 300 *kHz*, 3 μm pitch, 447 layers

Scalability

In general the presented structuring strategy and process should be scalable when the fluence and the pitch are kept constant. For higher average powers therefore the repetition rate and the marking speed has to be raised accordingly. In principal the scalability can be limited by two factors, first the marking speed of the scanning shows a highest value which defines a maximum repetition rate when the pitch is kept constant. Second a part of the energy of each pulse is always deposited as heat in the material. If the average power is too high compared to the structure dimensions heat accumulation will lead to melting effects and will reduce the surface quality. But today usually the scanning system represents the constraining factor as illustrated in Fig. 15. Here the machined Tux is shown for different average powers i.e. repetition rates and marking speeds but at the optimum pulse energy given by (5). In the top row the repetition rate is raised from 300 *kHz* to 500 *kHz*, 700 *kHz* and 1000 *kHz* for 532 *nm*. The average power directly scales with the repetition rate and amounted 120 *mW* at 300 *kHz* and 410 *mW* at 1000 *kHz*. Here the spot size and the pitch amounted 6.7 μm (f = 100 *mm* objective) and 3 μm, respectively. Higher average powers were finally impeded by the maximum marking speed of 3 *m/s*. The bottom row of Fig. 15 the same experiment but for a wavelength of 1064 *nm*, with a spot radius of w_0 = 16.3 μm (f = 160 *mm* objective) and a pitch of 8 μm. From left to right the repetition rate and average power was raised from 100 *kHz* with 925 *mW* to 200 *kHz* with 1.85 *W*, 300 *kHz* with 2.76 *W* and 600 *kHz* with 5.56 *W*. The marking speed is raised from 0.8 *m/s* at 100 *kHz* up to 4.8 *mm/s* at 600 *kHz* which was again the limit for the used scanner tuning.

For both sequences the machined structures were cleaned with a CO_2 flow and no other post processing were done. For each sequence no significant difference in the surface quality was observed i.e. the strategy and the process is scalable and with a faster scanner even structuring with higher powers should be possible.

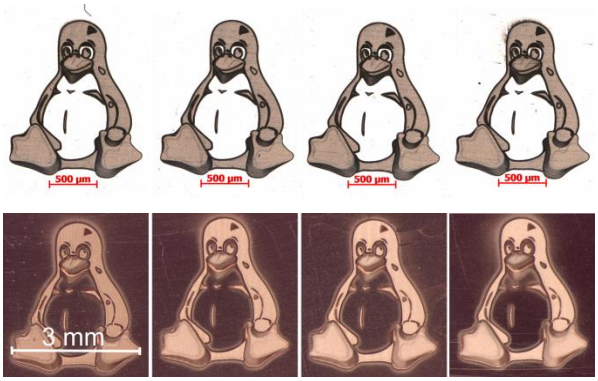

Fig. 15: Sequence of machined Tuxes. The average power and marking speed is enlarged form left to right. Top row: $\lambda = 532\ nm$, $w_0 = 6.7\ \mu m$, pitch 3 μm. Bottom row: $\lambda = 1064\ nm$, $w_0 = 16.3\ \mu m$, pitch 8 μm.

Periodical surface structuring

With the synchronized system it is possible to arrange craters with a given distance between each other. For one layer one pulse per cavity shot. In fig. 15a a pattern with 100 pulses per cavity is shown. The average power was 120 *mW* at a repetition rate of 300 *kHz* and the used pitch was 1 μm. In the normal asynchronous system the scanner would move to the first cavity, machine the crater and moves then to the next position. With the synchronized system, the used bitmap has been scanned, and always when a white pixel appeared, a laser pulse was released. By using 100 layers the bitmap has been scanned 100 times. At the end at every white pixel a cavity occurs. With this synchronized set up the machining of the cavities is much more efficient, because the acceleration before and after the ablation of one crater falls away. In fig. 16 another pattern with a detail view is shown. It can clearly be seen that all pulses strikes at the same point with a high accuracy concerning the position, during the movement of the synchronized scanner. Other periodical structures are shown in fig. 15 b,c where hexagonal combs or cubes (based on a hexagonal structure) were machined. The combs and cubes are performed with a pitch of 3 μm, an average power of 120 *mW*, a repetition rate of 300 *kHz* and 30 layers.

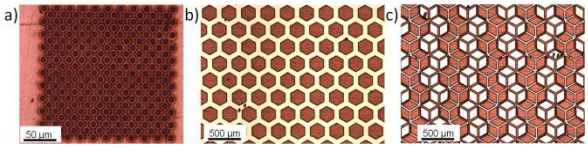

Fig. 15: Periodical surface structuring: a) cavity pattern; b) comb pattern; c) cube pattern based on a hexagonal structure

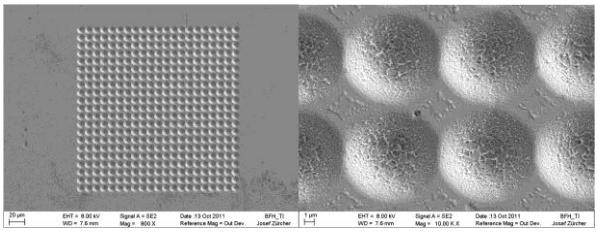

Fig. 16: SEM images of a cavity pattern with a detail view, 120 *mW*, 300 *kHz*, 100 layers

Summary and Outlook

The synchronization of mechanical components, here a galvo scanner, on the laser clock is shown and compared with the normal asynchronous motion of the scanner mirrors. A minimum R_a-value of about 90 *nm* can be achieved with a pitch of half of a spot radius for both systems the synchronized and the asynchronous scanner as well.

The minimum structures dimensions measured at the top of the structure amounts about a half to one spot radius for both strategies. But steep taper angles without deep marks at the bottom are only achieved with the synchronized set up i.e. this set up well suited to machine very precise structures.

A periodical pattern of craters with very high accuracy can be machined with continuous motion of the scanner mirror. This is significantly more efficient than the standard method where the mirror is stopped at each position of a crater.

At the moment the efficiency is limited by the speed of motion of the scanner mirrors. With another tuning of the mirrors it could be possible to gain about a factor of two. For faster micro machining, new beam control system with higher marking speeds should be tested.

The precision is limited by the optical system i.e. the spot radius. This problem could be avoided by using an axicon as a focusing lens and high precision axes which is reported in Michalowski et al [13], but one has to have in mind that in this case a significant part of the energy is lost.

Acknowledgements

This work is supported in parts by the Bern University of Applied Sciences Engineering and Information Technology and the Swiss Commission for Technology and Innovation CTI.

References

[1] S. Nolte, "Mikromaterialbearbeitung mit ultrakurzen Laserpulsen", Dissertation, Duvillier Verlag, Göttingen,

[2] S. Nolte, C. Momma, H. Jacobs, A. Tünnermann, B.N. Chichkov, B. Wellegehausen et al., "Ablation of metals by ultrashort laser pulses", J. Opt. Soc. Am. B / Vol 14, No. 10 / October 1997

[3] C. Körner, "Theoretische Untersuchungen zur Wechselwirkung von ultrakurzen Laserpulsen mit Metallen", Dissertation der technischen Fakultät der Universität Erlangen-Nürnberg, 1997

[4] B.N. Chichkov, C. Momma, S. Nolte, F. von Alvensleben, A. Tünnermann, "Femtosecond, picosecond and nanosecond laser ablation of solids", Appl. Phys. A 63, 109-115 (1996)

[5] C. Momma, S. Nolte, B.N. Chichkov, F. v. Alvenleben, A. Tünnermann, "Precise laser ablation with ultrashort pulses", Appl. Phys. Sci. 109/110, 15-19 (1997)

[6] C. Momma, B.N. Chichkov, S. Nolte, F. von Alvensleben, A. Tünnermann, H. Welling et al., "Short-pulse laser ablation of solid targets", Opt. Commun. 129, 134-142 (1996)

[7] B. Jaeggi, B. Neuenschwander, M. Schmid, M. Muralt, J. Zuercher and U. Hunziker, "Influence of the Pulse Duration in the ps-Regime on the Ablation Efficiency of Metals", Physics Procedia 12, 164-171 (2011)

[8] M. Schmid, B. Neuenschwander, V. Romano, B. Jaeggi and U. Hunziker, "Processing of metals with ps-laser pulses in the range between 10ps and 100ps", Proc. of SPIE Vol. 7920, paper 792009, (2011)

[9] B. Neuenschwander, B. Jaeggi, M. Schmid, U. Hunziker, B. Luescher, C. Nocera, "Processing of industrially relevant non metals with laser pulses in the range between 10 ps and 50 ps", ICALEO 2011, Paper M103 (2011)

[10] B. Neuenschwander, G. Bucher, G. Hennig, C. Nussbaum, B. Joss, M. Muralt, S. Zehnder et al., "Processing of dielectric materials and metals with ps laserpulses", ICALEO 2010, Paper M101 (2010)

[11] G. Raciukaitis, M. Brikas, P. Gecys, B. Voisiat, M. Gedvilas, "Use of High Repetition Rate and High Power Lasers in Microfabrication: How to keep Efficiency High? ", JLMN Journal of Laser Micro/Nanoengineering; Vol. 4 (3), p186-191 (2009)

[12] B. Neuenschwander, G. Bucher, C. Nussbaum, B. Joss, M. Muralt, U. Hunziker et al., "Processing of dielectric materials and metals with ps-laserpulses: results, strategies limitations and needs", Proceedings of SPIE vol. 7584, (2010)

[13] A. Michalowski, C. Freitag, R. Weber and T. Graf, "Laser surface structuring with long depth of focus", Proc. SPIE Vol. 7920, paper 79200W (2011)

[14] http://www.wikipaintings.org/en/m-c-escher/birds

[15] http://britton.disted.camosun.bc.ca/jbtess97.htm

[16] http://www.zazzle.ch/rosen_lithographie_fotoskulptur-153582013095294502

[17] http://wandtattoos.solineo.ch/shop/index.php?popup_box=images&pID=90020&products_id=90020&page=2

[18] http://en.wikipedia.org/wiki/File:Tux.svg

[19] http://brettworks.com/2012/04/26/on-the-musicality-of-m-c-escher/

[20] Bundesamt für Landestopographie swisstopo